Surface emissions modulate indoor SVOC concentrations through volatility-dependent partitioning

David M. Lunderberg [,1,2], Kasper Kristensen [2,a], Yilin Tian [2,3], Caleb Arata [1,2], Pawel K. Misztal [2,c], Yingjun Liu [2,b], Nathan Kreisberg [4], Erin F. Katz [5], Peter F. DeCarlo[6], Sameer Patel[7], Marina E. Vance [7], William W Nazaroff [3], and Allen H. Goldstein [2,3]*

[1] *Department of Chemistry, University of California, Berkeley, CA, USA.*
[2] *Department of Environmental Science, Policy, and Management, University of California, Berkeley, CA, USA.*
[3] *Department of Civil and Environmental Engineering, University of California, Berkeley, CA, USA.*
[4] *Aerosol Dynamics Inc., Berkeley, CA, 94710, USA*
[5] *Department of Chemistry, Drexel University, Philadelphia, Pennsylvania, USA*
[6] *Department of Environmental Health and Engineering, Johns Hopkins University, Baltimore Maryland 21218*
[7] *Department of Mechanical Engineering, University of Colorado Boulder, Boulder, CO, USA.*

[a] *Now at Department of Engineering, Aarhus University, Denmark*
[b] *Now at BIC-ESAT and SKL-ESPC, College of Environmental Sciences and Engineering, Peking University, China*
[c] *Now at Department of Civil, Architectural and Environmental Engineering, The University of Texas at Austin, Austin, TX, USA*
[*] *Corresponding email: david_lunderberg@berkeley.edu*

0 ABSTRACT

Measurements by semivolatile thermal desorption aerosol gas chromatography (SV-TAG) were used to investigate how semivolatile organic compounds (SVOCs) partition among indoor reservoirs in (1) a manufactured test house under controlled conditions (HOMEChem campaign) and (2) a single-family residence when vacant (H2 campaign). Data for phthalate diesters and siloxanes suggest that volatility-dependent partitioning processes modulate airborne SVOC concentrations through interactions with surface-laden condensed-phase reservoirs. Airborne concentrations of SVOCs with vapor pressures in the range of C13 to C23 alkanes correlated with indoor air temperature. Observed temperature dependencies were quantitatively similar to theoretical predictions that assumed a surface-air boundary layer with equilibrium partitioning maintained at the air-surface interface. Airborne concentrations of SVOCs with vapor pressures corresponding to C25 to C31 alkanes correlated with airborne particle mass concentration. For SVOCs with higher vapor pressures, which are expected to be predominantly gaseous, correlations with particle mass concentration were weak or nonexistent. During primary particle emission events, enhanced gas-phase emissions from condensed-phase reservoirs partition to airborne particles, contributing substantially to organic particulate matter. An emission event related to oven-usage was inferred to deposit siloxanes in condensed-phase reservoirs throughout the house, leading to the possibility of reemission during subsequent periods with high particle loading.

1 INTRODUCTION

In indoor environments, semivolatile organic compounds (SVOC) dynamically partition between the gas phase and various condensed-phase reservoirs, such as airborne particles, surface films, settled dust, and building materials.[1] Many specific indoor SVOCs are of concern for human health, such as endocrine-disrupting phthalate diesters and halogenated flame retardants.[2] Airborne particles are often partly composed of SVOCs. Exposure to particulate matter is among the leading global mortality risk factors,[3] although the specific roles of SVOCs and the relative importance of indoor particle exposure contributing to this risk are unknown. Understanding the

dynamics and physical behavior of indoor airborne SVOC concentrations is important for risk assessment and exposure mitigation.

Emerging evidence indicates that interactions between indoor air and condensed-phase reservoirs influence airborne SVOC concentrations. Surface reservoirs are defined as "condensed-phase materials containing chemical constituents that undergo exchange with the gas phase."[4] Recent field measurements of volatile organic compounds (VOCs) and SVOCs in real indoor settings suggest that organics readily desorb from condensed-phase reservoirs into bulk air. The high rate of desorption suggests that, for many compounds, the condensed-phase reservoirs are either interior surface films or thin layers of building materials closely in contact with indoor air.[4-8] Weschler and Nazaroff described a model for the growth of SVOC-laden organic surface films indoors and suggested that surface films may provide functional and chemical homogeneity among the diverse surfaces interacting with bulk indoor air.[9]

Models describing indoor surface emissions have assumed the existence of a boundary layer immediately adjacent to surfaces, with equilibrium partitioning maintained at the surface-air interface.[10-14] Emissions from surfaces are then regulated by the concentration difference across the boundary layer combined with a convective mass transfer coefficient that limits mass transfer between the boundary layer and bulk air. In a chamber study of vinyl flooring, Clausen et al. noted that temperature was a primary factor controlling diethyl hexyl phthalate (DEHP) emissions.[14] Temperature changes affect equilibrium partitioning between the gas-phase and condensed-phase surface reservoirs, including surface films. Such processes have been characterized using thermodynamic models.[15-18]

Airborne particles may significantly influence SVOC emission rates from surfaces by transporting SVOC mass out of the boundary layer and/or by providing an airborne condensed-phase sink.[19] Chamber studies of organophosphate flame retardants and plasticizers have demonstrated similar partitioning phenomena whereby the presence of airborne particles enhances the rate of SVOC emissions from source materials.[20-22] Moreover, the affinity of SVOCs for airborne particles is affected by both SVOC and particle composition for phthalate diesters[22,23] and for third-hand smoke (THS) species.[24] These findings have been supported by measurements in real indoor environments for specific compounds. For example, in a study of a university classroom, DeCarlo et al. reported that increases in particle mass concentration led to increases in the concentrations of airborne THS species; they inferred that surface-sorbed THS species were transported through the gas phase onto aqueous airborne particles, with particle capacity influenced by acid-base processes.[25] Similarly, increases in DEHP concentrations were found to be associated with increased airborne particle concentrations in a normally occupied residence.[8]

Indoor environments are subject to dynamic changes in temperature and particle concentration as influenced by occupants, their activities, and building interactions with the outdoor environment. Indoor airborne SVOC concentrations may be modulated by both direct primary emissions and by indirect interactions with surfaces. Few studies have examined how airborne SVOC concentrations evolve in real indoor settings. In this paper, we report hourly SVOC concentrations from two field campaigns, H2 and HOMEChem, and we use these data to characterize SVOC volatility-dependent dynamics and partitioning. We focus on three specific

species groupings: (a) total SVOC concentrations binned by volatility, (b) phthalate diesters, and (c) cyclic siloxanes. These emphases are intended to explore SVOC behavior as a bounded class and as discrete compounds with varying vapor pressures. The specific objectives of the study are: (a) to quantitatively describe indoor SVOC dynamics as functions of volatility, temperature, and particle loading; (b) to connect observations with predictions from theory and laboratory experiments; and (c) to evaluate the impact of surface emissions on airborne SVOC concentrations.

2 EXPERIMENTAL METHODS

Data analysis from the H2 observational field campaign focuses on a period of vacancy in an otherwise normally occupied residence. At H2, SVOC concentrations are binned by volatility and compared against temperature and particle mass concentrations. The HOMEChem campaign was structured around controlled occupant activities in a research house. At HOMEChem, the physical behavior of two classes of compounds, phthalate diesters and cyclic siloxanes, is investigated in relation to their volatility.

Study Sites: The H2 field campaign was conducted a single-family dwelling in Contra Costa County, California, from 7 December 2017 to 4 February 2018. In this residence, air temperature was regulated by a forced-air gas-fired furnace incorporating a MERV 13 filter that influenced indoor particle levels. The furnace operated under control of a programmable thermostat, with "on" periods occurring twice daily (06:45–07:15 and 17:45–22:00). The H2 site and field monitoring campaign are detailed elsewhere.[7,8] The analysis here focuses on a five-day period (22-27 December) during which the house was unoccupied (the H2 'vacant period').

The HOMEChem field campaign was conducted during June 2018 at the UTest House, a manufactured house located at the JJ Pickle Research Campus of the University of Texas at Austin. The three-bedroom, 111-m^2 facility was operated with an air-conditioning system set to maintain a constant indoor air temperature of ~25 °C (298 K). A series of controlled experiments was conducted over the one-month campaign. Experiments were designed to explore the influence of cooking, cleaning, and occupancy on indoor air chemical composition. Two categories of experiments were undertaken. During 'sequential' experimental days, repeated 'stir fry cooking' or 'cleaning' experiments were conducted with intermittent venting periods to reset indoor conditions. 'Layered' experimental days simulated 'day-in-the-life' conditions for a residence, with meal preparation and cleaning occurring in a sequential manner without venting. Two high-emission 'layered' days were conducted to simulate 'Thanksgiving,' with more intensive cooking and occupancy of the type typical of the holiday meal in an American household. A full description of the HOMEChem campaign experimental design and an overview of all instrumental data acquisition is reported elsewhere.[26]

Instrumentation and Measurement Methods: The research reported here focuses on data acquired using semivolatile thermal desorption aerosol gas chromatography (SV-TAG), a dual-channel gas chromatograph mass spectrometer (GC-MS) that quantifies, with hourly time resolution, gas-phase and gas-plus-particle-phase concentrations of SVOCs with vapor pressures corresponding to alkanes between ~C14 and ~C35.[27-29] SV-TAG collected the $PM_{2.5}$ particle fraction, excluding larger particles by means of a cyclone (BGI by Mesa Labs, SCC 2.654). After each sampling period (15 minutes at H2, 20 minutes at HOMEChem), the captured analytes are

thermally desorbed from the collection cells, separated based on volatility using a gas chromatograph (Agilent 7890A) and analyzed using a 70-eV electron ionization (EI) mass spectrometer (Agilent 5975C). Measurements are repeated automatically at hourly intervals. SV-TAG was deployed during the H2 and HOMEChem campaigns. Operating and sampling parameters during the H2 campaign are described in the SI (Table S1) and in prior publications.[7,8] Operating parameters during the HOMEChem campaign were unchanged from the H2 campaign. Sampling parameters during HOMEChem are described in Table S2 and in Farmer et al.[26] Characteristic ions of most species were integrated using the TERN software, normalized to relevant internal standards, and calibrated against authentic external standards.[30] Quantification of low-volatility siloxanes (Figure S1), for which authentic external standards were not available, is described in the SI.

At HOMEChem, particle number concentrations were quantified by two separate scanning mobility particle sizers, with one implementing a nano differential mobility analyzer (4-105 nm: TSI 3080 EC + 3085 nano-DMA + 3788 water CPC) and one implementing a long differential mobility analyzer (105-532 nm: TSI 3080 EC + 3081 long-DMA + 3787 water CPC). Size-resolved concentrations of larger particles (diameter > 542 nm) were determined by an aerodynamic particle sizer (TSI 3321). At H2, particle number concentrations were quantified by a Grimm 11-A optical particle counter reporting time-resolved measurements in 31 size-segregated bins with particle diameters ranging from 0.25 to 32 μm. For the HOMEChem study, an assumed particle density of 1 g cm^{-3} (similar to the density of cooking-related aerosol) was used for consistency with other work.[31,32] The present work similarly assumed a particle density of 1 g cm^{-3} at the H2 site for internal consistency. (A density of 1.67 g cm^{-3} was assumed in prior published work at the H2 site.[8,33,34]) The presence of particle-bound siloxanes was confirmed with supporting measurements from a high-resolution time-of-flight aerosol mass spectrometer (HR-ToF-AMS), with experimental details available in the SI (Figure S2).

SVOC Integration: The chromatographic signal from SV-TAG was converted into total SVOC concentrations following the approach of Kristensen et al.[7] In the present work, the chromatogram was subdivided into bins where bin borders were defined by the midpoints of the retention times of adjacent alkanes. Then, each bin was normalized to the closest alkane internal standard in retention time and quantified using calibration curves prepared for the closest alkane in retention time (Figure 1). Normalization by internal standards is needed to account for a general decline in ion-source response (restorable by source-cleaning) and for matrix loading effects. Alkane-internal standards are used as the closest surrogate for each SVOC-bin in volatility space but may not be fully representative for highly polar compounds contained within each bin. The retention time is closely related to compound volatility, although other parameters, such as polar interactions with the column, can influence retention. Summing all bins and subtracting blank 'internal-standard only' measurements yielded the 'total SVOC' concentration. SV-TAG incorporates in-situ derivatization in its analytical procedure, which may affect the retention time of derivatized compounds. The derivatization agent, N-methyl-N-(trimethylsilyl)trifluoroacetamide (MSTFA), reacts with hydroxy groups such as carboxylic acids, alcohols, sugars, and similar analytes, and replaces active hydrogen atoms with trimethylsilyl groups. Silylation occurs for only a small subset of captured analytes and generally shifts the retention time by no more than 1-2 alkane-equivalent volatility bins. Most of the volatility bins are expected to be captured by the collection and thermal desorption (CTD) cell

with negligible loss through the collection and transfer processes. Collection efficiencies of gas-phase organics on the CTD cell are expected to be high (80-100% for most measured compounds). Transfer efficiencies off the CTD cell and focusing trap were > 95% for the C15 – C26 alkanes and decreased to 50% by the C32 alkane, while the transfer efficiency of the C14 alkane was 40%. The uncharacterized C13 alkane transfer efficiency is expected to be lower.[27] Quantitative corrections for transfer losses were made using deuterated alkane internal standards deposited on the CTD cell and analyzed with every sample.

Modeling Temperature Dependence of Gaseous SVOCs: Past models have been developed to estimate gas-phase SVOC concentrations in two separate cases.[35] In one case, SVOCs are emitted from surfaces when additive SVOCs are released from a parent material, such as in the case of plasticizers. Then, equation (1) describes the gas-phase concentration y, where h is the convective mass-transfer coefficient over the emission surface, y_0 is the gaseous SVOC concentration immediately adjacent to the surface, A is the source surface area, and Q^* is the "equivalent ventilation rate," a parameter related to the ventilation rate that accounts for particle-associated removal and is described more thoroughly in the SI.

$$y = \frac{h \times y_0 \times A}{h \times A + Q^*} \qquad (Eq.1)$$

In another case, SVOCs can be emitted from surfaces when a previously sorbed or otherwise deposited SVOC is released from that surface, such as in the case of pesticide or water-repellant treatments. This process occurs over two phases. For each phase, equation (2) describes the gas-phase SVOC concentration, where A_s refers to the sorbing interior surface area and h_s is the convective mass-transfer coefficient over interior surfaces.

$$y = \frac{h \times y_0 \times A}{h \times A + h_s \times A_s + Q^*} \qquad (Eq.2)$$

Under variable temperature, changes in y across the observed temperature range (288 – 292 K) are assumed to be governed by changes in the equilibrium constant controlling y_0, as described in equation (3) where $[SVOC_{\text{surf}}]$ is the condensed-phase SVOC concentration at the surficial interface.

$$K_{\text{eq}}(T) = \frac{y_0}{[SVOC_{\text{surf}}]} \qquad (Eq.3)$$

Such changes in equilibrium partitioning are anticipated to be similar to those described by the van't Hoff equation as shown in equation (4), where T is temperature, ΔS is the entropy of vaporization, R is the gas constant, and k is a constant described by $-\Delta H/R$, where ΔH is the heat of vaporization.[18]

$$K_{\text{eq}}(T) = \exp\left[\frac{\Delta S}{R} + k\left(\frac{1}{T}\right)\right] \qquad (Eq.4)$$

We present a model describing gas-phase SVOC concentrations based on the framework developed in equations (1-4). Then, y as a function of temperature is described by equation (5), where a is a variable containing terms that are generally independent of temperature. A full derivation of equation (5) is available in the SI. Because the van't Hoff equation applies to equilibrium partitioning of a pure material and the studied indoor physical system consists of a complex mixture, we refer to experimentally derived k values as k^*.

$$y(T) = a \times \exp\left[k^*\left(\frac{1}{T}\right)\right] \qquad (Eq.5)$$

3 RESULTS AND DISCUSSION

At H2, SVOC concentrations were determined for chromatographic bins corresponding to the volatility of the nearest alkane in retention time ('alkane-equivalent volatility bin'). Estimated vapor pressures and saturation concentrations (C^*) for each bin are reported in Table S3. Concentrations are reported for the vacant period when no occupant activities, such as cooking or cleaning, occurred. Departures from steady-state conditions during the vacant period are likely to occur with (1) controlled indoor temperature changes related to the home heating system and (2) changes in indoor air $PM_{2.5}$ concentrations. During the period of vacancy, indoor primary particles are expected to originate only from infiltration of outdoor particles and not from any indoor source.[8] Observed dynamic behavior of SVOCs was separated into two categories based on volatility: the C13-C23 bins, which are predominantly gaseous and display dependence on temperature, and the C25-C31 bins, which partition appreciably into airborne particles and display dependence on particle concentration.

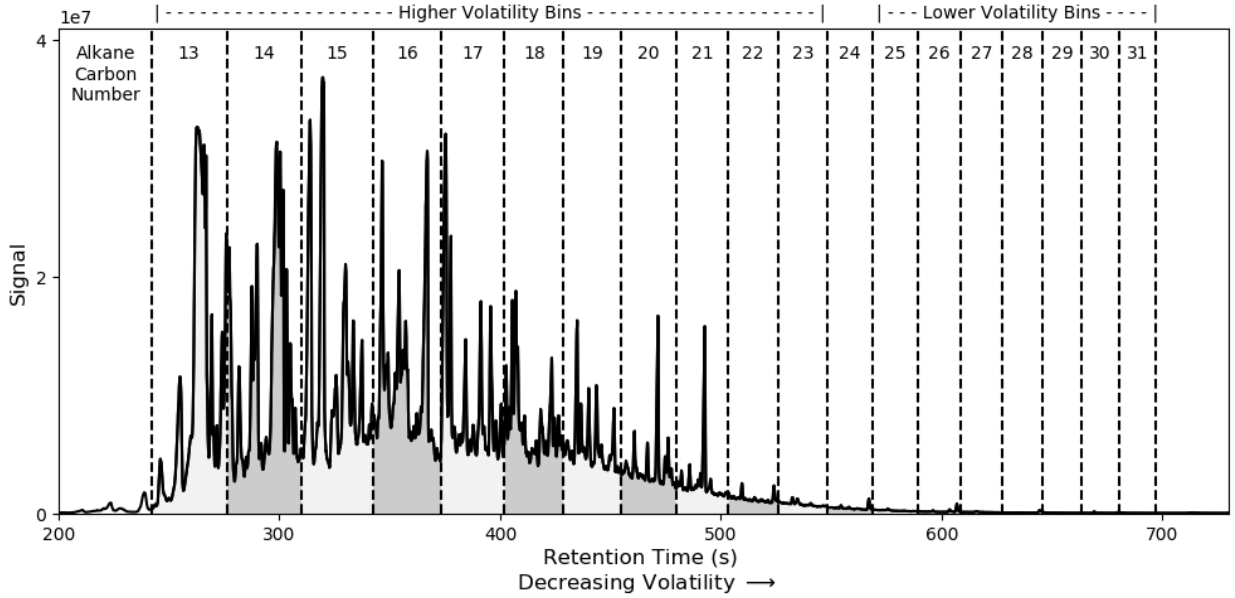

Fig. 1. Quantified bins of the SV-TAG chromatogram are displayed for a typical chromatogram. Bins were subdivided and quantified based on the closest alkane in retention time.

Abundance of Higher Volatility SVOCs is Associated with Temperature. During the vacant period at H2, observed total (gas-plus-particle) SVOC concentrations of the C13-C23 bins generally decreased with decreasing volatility. Average concentrations and associated summary

statistics of each alkane-equivalent volatility bin are reported in Table S3. Concentrations in the C23 bin were roughly fifty times lower than concentrations in the C13 bin. In Figure 2, SVOC concentrations are compared binwise against indoor air temperature, with ordinary least squares regression lines superimposed. For the C13-C23 bins (C13-C22 shown), SVOC concentrations showed statistically significant positive variation with temperature. Furthermore, the magnitude of the fitted slopes tended to decrease with decreasing bin volatility. Significant positive variation with temperature was not observed beyond the C23 bin. Time series and comparisons against temperature for each bin are shown in the SI (Figures S3, S4).

Observed temperature dependencies can be connected to the model described in equation (5). Predicted k^* values were calculated from literature values for alkane heats of vaporization, which correlate with vapor pressure.[37,38] Experimental k^*values are within 50% of predicted k^* values, a remarkably close correspondence (Figure S5). Discrepancies between the two values may arise because the vapor pressures of the measured organics differ from alkane vapor pressures and because the studied system involves vaporization from a complex mixture rather than from a pure condensed phase. Furthermore, the application of equation (5) requires that emissions from surfaces are the dominant source process. Larger differences between the experimental and predicted values of k^* are observed for the C21 and C22 alkane-equivalent volatility bins. Other factors, such as appreciable interactions with airborne particles, are expected to partially account for this observation.

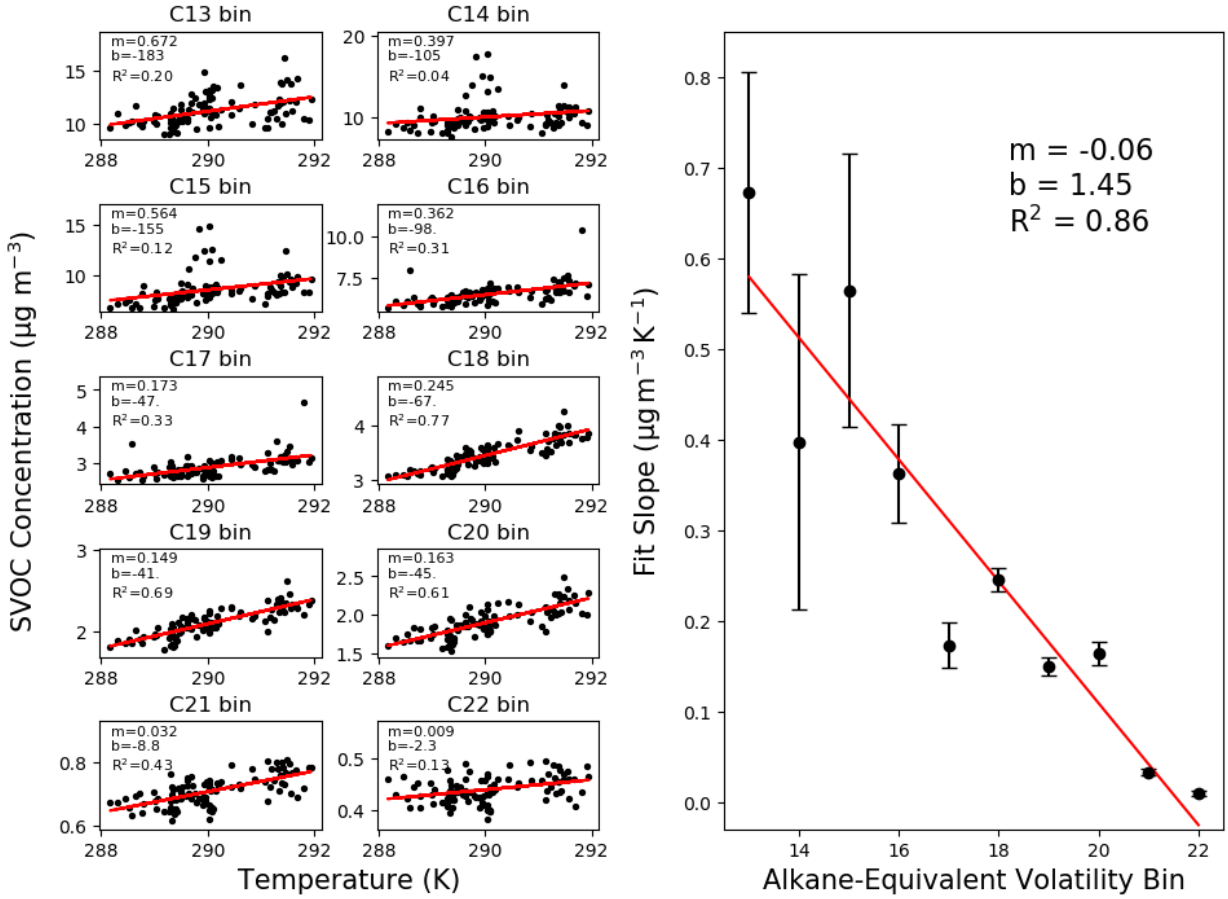

Fig. 2. In the left panel, total (gas-plus-particle) SVOC concentrations (µg m^{-3}) are compared against temperature. Each measured point represents a 15-minute sample collection period with hourly replication during the observational period. Units of measure for the linear fit slope and intercept are µg K^{-1} m^{-3} and µg m^{-3}, respectively. In the right panel, the magnitude of the linear fit slope is compared against the corresponding alkane-equivalent volatility bin.

Abundance of Lower Volatility SVOCs is Associated with Particle Concentration. During the vacant period at H2, consistent associations between total airborne SVOC concentrations and particle mass concentration were observed for the C25-C31 bins (Figure 3). We stress that SV-TAG samples only the $PM_{2.5}$ particle fraction; coarse-mode particles (as observed during resuspension events) likely have a different chemical composition than $PM_{2.5}$, which may alter equilibrium partition behavior. Furthermore, equilibration time scales are slower for larger particles and faster for smaller particles. As such, equilibration is less likely to be achieved during the time of indoor suspension for coarse particles as compared to fine particles.[36] Time series and comparisons against particle mass concentrations for each bin are shown in the SI (Figures S3, S6). These bins had substantial fractions (~0.4 to ~1.0) of airborne mass in the particle-phase (Table S3). Conversely, positive associations between SVOC concentrations and particle mass concentration were not observed for the C13-C23 bins. SVOCs contained in these higher volatility bins were predominantly in the gas-phase and are not expected to strongly partition to particles. The intercepts of the ordinary least-squares fits displayed in Figure 3 are

related to the airborne gas-phase concentration in the absence of particles. As SVOC volatility decreases, the background gas-phase SVOC concentration generally decreases. Gas-particle partitioning by bin is displayed in Figure S7. As expected, the observed particle fraction, F_p, generally increases with increased particle mass concentration and with decreased vapor pressure.

The strong correlation ($R^2 > 0.4$) between $PM_{2.5}$ and the airborne SVOC concentrations in the C25-C31 bins suggests a net outcome of surface-particle partitioning as SVOCs are transported from condensed-phase reservoirs. We infer that the gas-phase acts as a transport medium between condensed-phase SVOC surface reservoirs and airborne particles. Gas-phase SVOC concentrations were relatively constant under variable particle concentrations considering experimental uncertainty (Figure S8). Correlations between $PM_{2.5}$ and SVOC concentrations for bins below C25, which are predominantly in the gas-phase, were weaker ($R^2 < \sim 0.3$) or not observed (Figure S6).

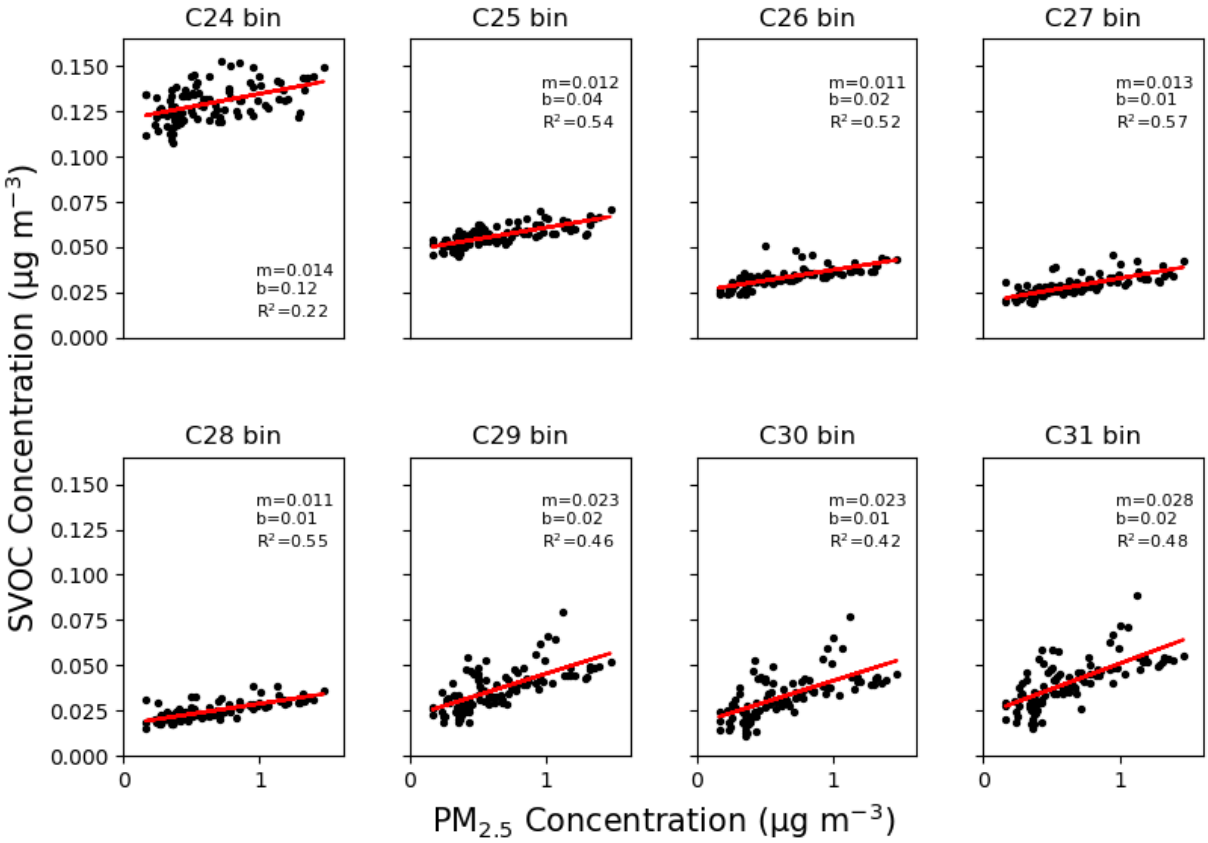

Fig. 3. Binned total (gas-plus-particle) SVOC concentrations (µg m^{-3}) are compared against $PM_{2.5}$ mass concentrations (µg m^{-3}) at H2 during the vacant period. The linear fit slope (*m*) is dimensionless; the intercept (*b*) has units of µg m^{-3}. Each measured point represents a 15-minute sample collection period with hourly replication during the observational period.

Infiltration of outdoor gas- and particle-phase SVOCs as well as changes in source emission rates may also influence observed concentrations in indoor air. Indoor-outdoor concentration ratios of the alkane-equivalent volatility bins were slightly below unity with moderate variability (Figure S9). However, because outdoor particle mass concentrations were greater than indoor particle mass concentrations, SVOC concentrations per particle mass were greater indoors than outdoors. As indoor particles during the H2 vacant period are expected to be primarily of outdoor origin,[8] this evidence suggests the occurrence of net partitioning of indoor SVOCs to outdoor particles upon transport to the indoors. Particle-normalized indoor/outdoor ratios of alkane-equivalent volatility bins display substantial variability, whereas indoor SVOC concentrations were highly regular. The regular correspondence between SVOC concentrations and $PM_{2.5}$, coupled with high normalized indoor/outdoor ratios, suggests that partitioning processes may be modulating observed indoor SVOC concentrations at time scales comparable to or faster than the air-exchange rate. Under classical partitioning theory, it is assumed that SVOCs partition by absorption into the organic $PM_{2.5}$ fraction rather than by adsorption to bulk particle surfaces.[15]

Indirect Surface Emissions Contribute to Indoor Particle Mass. During the first HOMEChem 'Thanksgiving' experiment, substantial proportions of airborne $PM_{2.5}$ mass originated from primary cooking emissions. Among primary species emitted are palmitic acid, stearic acid, and other carboxylic acids with varying degrees of unsaturation. Such species have been reported to be directly emitted from cooking in laboratory studies.[40-42] We also found that squalene emissions were strongly associated with oven usage on Thanksgiving; the expected source is volatilization of oils from the skin of the roasting turkey. An additional source could be from human skin oils present on heated surfaces or cookware. Squalene was observed during other cooking events at roughly one-to-two orders of magnitude smaller abundance.

Surprisingly, we also observed on this day elevated indoor particle-phase concentrations of specific SVOCs that should not originate from the food itself, in particular phthalates, adipates, and siloxanes (Figure 4, Figures S1, S2). Phthalates and adipates are plasticizers commonly used in vinyl flooring.[43] Low-volatility siloxanes are used as thermally stable lubricating greases and sealants. Remarkably, plasticizer and siloxane concentrations accounted for approximately 10% of airborne particle mass at certain times on this experimental day, suggesting that partitioning processes between particles and condensed-phase reservoirs significantly influenced the observed airborne concentrations. Moreover, these observations highlight difficulties in determining exact SVOC emission profiles of events in a real-world setting: surface emissions that were indirectly stimulated by primary event-driven particle emissions contributed sizeable fractions of indoor $PM_{2.5}$ mass.

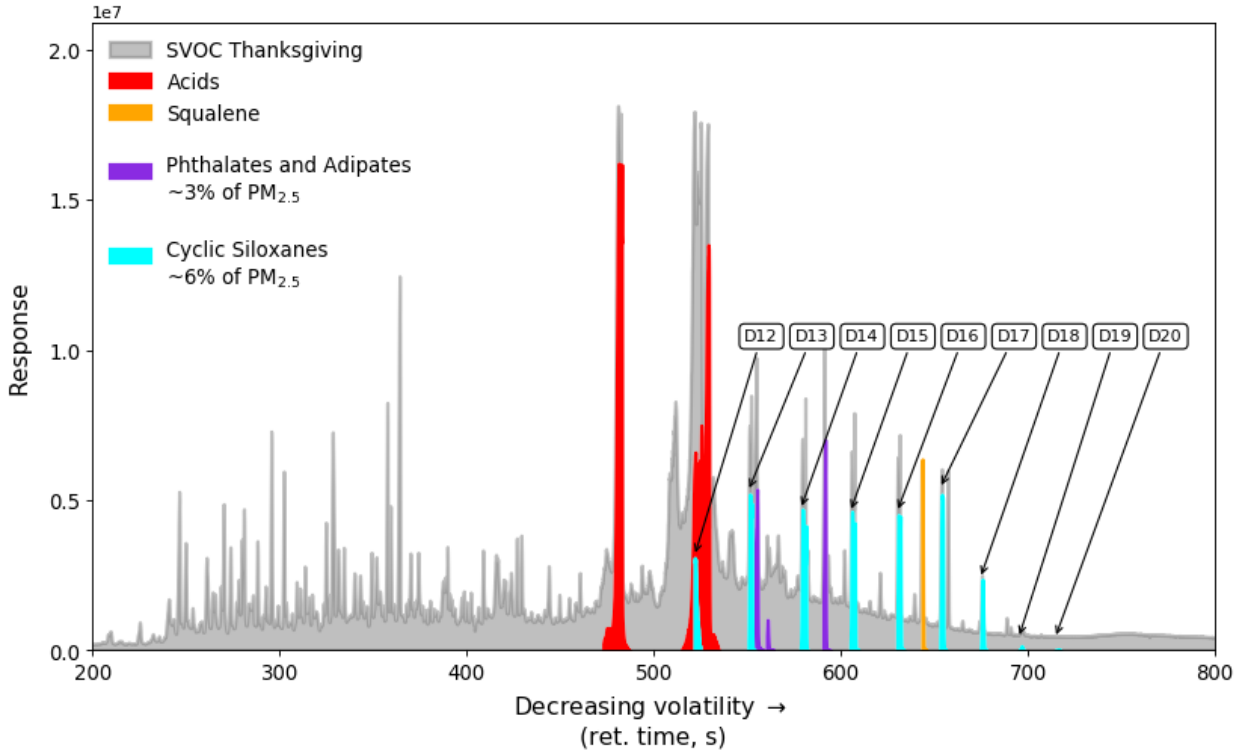

Fig. 4. A particle-phase chromatogram from the first 'Thanksgiving' experiment day ($PM_{2.5}$ concentration = 245 μg m^{-3}) on June 18 at 3:05 PM is displayed. Direct emissions attributable to cooking (carboxylic acids and squalene) are highlighted in red and orange, respectively. Indirect emissions likely attributable to the building composition are highlighted in purple (plasticizers) and teal (siloxane lubricants and heat-transfer materials).

In previous analyses of data from the H2 field campaign, correlations between particle mass concentration and airborne DEHP concentration suggested that particulate matter rapidly acquired surface-laden DEHP from reservoirs such as organic surface films and dust.[8] Prior analysis of airborne DEHP concentrations at the UTest House characterized the role of temperature over a 9 K range.[44] In that case, on a long-term basis, a 9 K increase in temperature approximately doubled airborne DEHP and butyl benzyl phthalate (BBzP) concentrations. However, there was no systematic examination in that study of particle-dependent variations in phthalate concentrations. In the current work at the UTest House, with temperature approximately constant at 298 K, strong associations between particle concentration and total airborne SVOC concentrations were observed for both DEHP and BBzP (Figure 5).

Substantial portions of the UTest House vinyl flooring are known to contain phthalates.[44] Because both DEHP and BBzP are expected to originate from the composition of the flooring material, and because airborne phthalate concentrations are strongly associated with particle concentration for many different source events, it is similarly inferred that transport through the gas phase from condensed-phase stationary reservoirs to airborne particles is the principal source of observed particulate phthalate concentrations during the HOMEChem campaign. DEHP resides in the C25 alkane-equivalent volatility bin and BBzP resides in the C24 alkane-equivalent volatility bin based on chromatographic retention time.

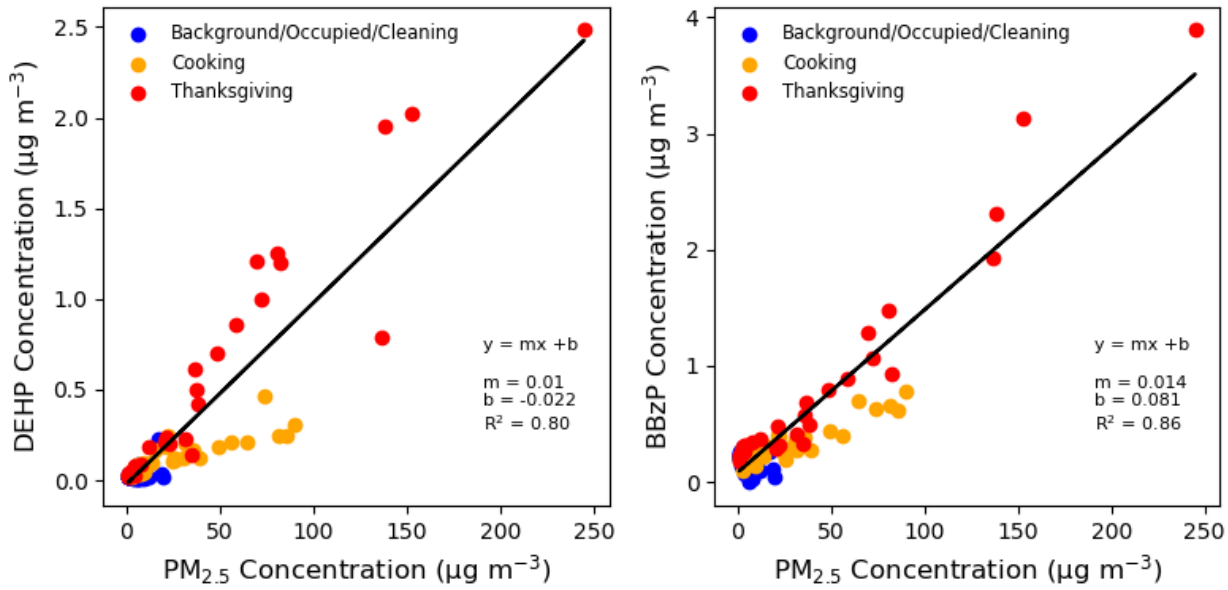

Fig. 5. Total (gas-plus-particle) concentrations (µg m^{-3}) of two phthalates, DEHP and BBzP, are compared against particle mass concentration (µg m^{-3}) for measurements from the HOMEChem campaign. Units of measure for the fit slope (*m*) and intercept (*b*) are unitless and µg m^{-3}, respectively.

Lower Volatility Siloxanes Exhibit Ongoing Emissions after High Emission Event. Surprisingly high concentrations of low-volatility siloxanes (D13-D20 cyclic and L13-L19 linear siloxanes) were observed during a particle loading event associated with the HOMEChem 'Thanksgiving' experiment day on June 18 in association with cooking and oven use. We hypothesize that the low-volatility siloxane source is the oven, an appliance that likely contains heat-transfer compounds and thermally stable lubricants. Commercially available products containing siloxanes have been recommended for such uses in ovens.[45] In principle, high temperatures attained throughout the oven during cooking could have driven appreciable amounts of low-volatility siloxanes into the gas-phase, which subsequently condensed onto airborne particles as air exited the oven and cooled. Although the oven was approximately thirteen years old, it had been operated only three times prior to the June 18 Thanksgiving event. Peak concentrations of low-volatility siloxanes during the 'Thanksgiving' experiment day are reported in Table S4. Minor siloxane enhancements were observed in the morning (stovetop breakfast preparation) and evening (oven cooking) of the June 8 layered day, but not during the lunch-time stir-fry event.

Small enhancements of D18 were observed during cooking events on the June 17 sequential stir-fry day; enhancements of other siloxanes were not observed. In contrast, D12-D14 siloxanes were strongly enhanced during cooking events on the June 19 'layered' experiment day. A plausible explanation for these observations is that siloxanes emitted during the June 18 'Thanksgiving' experiment day were deposited on surfaces throughout the residence and were subsequently reemitted during high particle emission events (Figure 6). Reemission of the semivolatile siloxanes occurred more readily for smaller homologues, which have correspondingly higher vapor pressures. Lower-volatility siloxanes are expected to preferentially partition to airborne particles; however, airborne concentration enhancements may not be

observed for species with especially low volatility, for which equilibration time scales are significantly longer than the particle residence time indoors.

The D12-D19 siloxanes reside in the C22-C31 alkane-equivalent volatility bins, suggesting that their physicochemical properties may be well suited for reemission from surfaces. Vapor pressures and octanol-air partition coefficient (K_{oa}) values for D12-D19 were calculated using SPARC and are reported in Table S5. Using the method of Weschler and Nazaroff[1] and assuming a condensing-particle diameter of 100 nm and a gas-phase diffusivity of 0.03 $cm^2\ s^{-1}$, gas-particle equilibration time scales for D12 are expected to be on the order of 8 days while equilibration time scales for D19 are expected to be effectively infinite (~ 10^9 y). A mechanical ventilation system was operated to maintain an air-exchange rate of ~0.5 per hour during the HOMEChem campaign.[26] The calculated vapor pressure of D12 ($10^{-12.1}$ atm) is similar in magnitude to that of DEHP ($10^{-11.85}$ atm), a compound that displayed prominent gas-particle interactions in a normally occupied residence.[8] The calculated vapor pressure of D19 is eight orders of magnitude lower. In summary, airborne concentration enhancements may occur for D12 in association with increased $PM_{2.5}$ loading but are not expected to occur for D19 without an additional stimulus, such as the inference that the high-temperature event associated with oven-use drove D19 into the gas-phase. Linear siloxanes, which were emitted at far lower concentrations during the June 18 Thanksgiving emission event, were not observed significantly above background during the June 19 layered day. Small siloxane enhancements were observed for D12-D16 siloxanes on the June 12 sequential stir-fry day. These observations may be related to deposition events from oven use on June 5 and June 8.

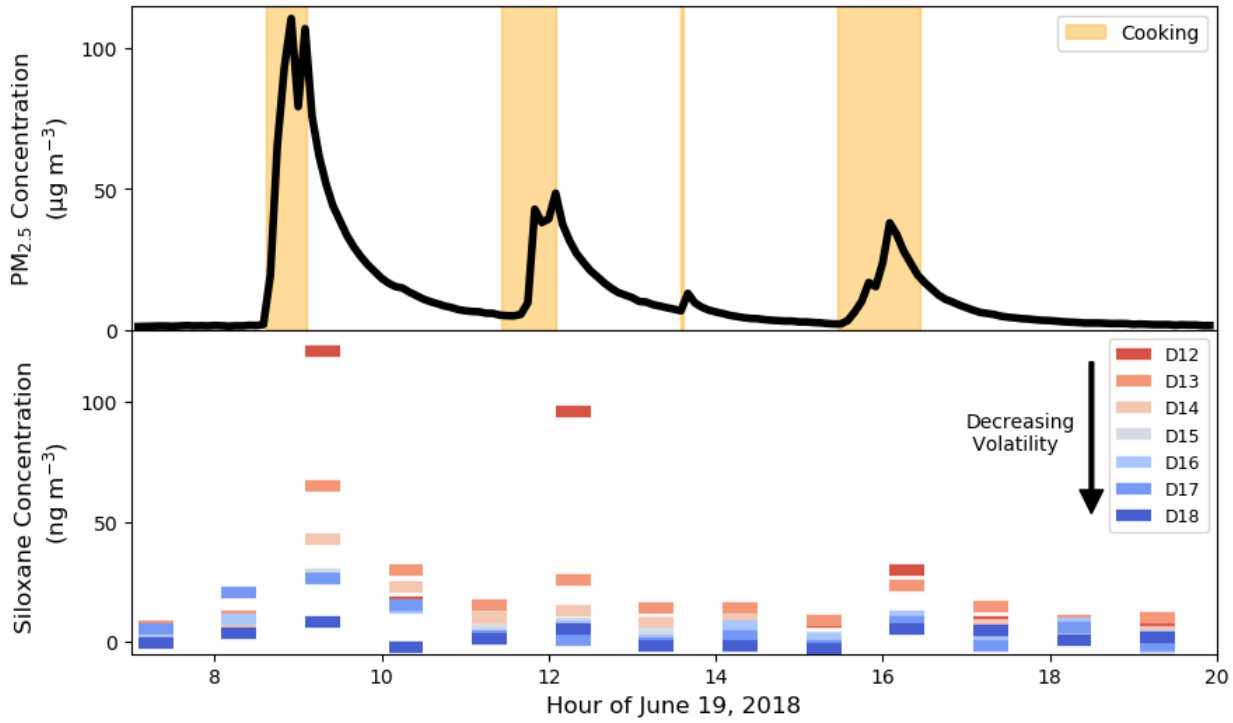

Fig. 6. Total (gas-plus-particle) airborne concentrations (µg m^{-3}) of a siloxane homologous series superimposed on $PM_{2.5}$ concentrations (µg m^{-3}) for a 'layered' experiment day on June 19 following the June 18 'Thanksgiving' experiment day.

Implications. In the absence of episodic emission sources, key driving factors influencing variability of indoor airborne SVOC concentrations are volatility and partitioning phenomena. Airborne concentrations of the higher volatility (C13-C23 bins; predominantly gaseous) SVOCs are mainly sensitive to surface temperatures. Concentrations of lower volatility (C25-C31 bins; substantially particle-phase) SVOCs are sensitive to airborne particle concentrations. This work suggests that, at the H2 residence, the dynamic behavior of specific SVOCs can be predicted if their volatility is known. Ultimately, if demonstrated to be generalizable, such understanding would contribute to improving exposure assessment and mitigation strategies.

Emissions of low-volatility siloxanes and phthalates from surfaces are inferred to have been indirectly stimulated by event-driven emissions of particles. Analysis of low-volatility siloxane concentrations suggests that SVOCs can be deposited throughout a residence and then reemitted during subsequent particle loading events. This effect was most important for siloxanes with significant particle-bound fractions and appreciable gas-phase fractions. Despite similar total (gas-plus-particle) airborne concentrations during the initial source event, smaller concentrations of lower volatility siloxanes were observed during reemission events compared to higher volatility siloxanes. Because indoor air is the transporting medium between condensed-phase surface reservoirs and airborne particles, the lowest-volatility siloxanes are expected to remain in condensed-phase reservoirs when considering kinetic transport limitations. These lowest-volatility siloxanes were observed during primary emission events involving oven use but not appreciably during reemission episodes.

These observations of airborne SVOC concentrations are consistent with, but not fully demonstrative of prior modeling and laboratory results. More work is needed to strengthen confidence in current models by connecting speciated measurements of surface-sorbed organics to airborne SVOC concentrations over longer time scales and in other indoor spaces. Future analysis would benefit from chemically differentiating primary event emissions and indirect event emissions where surface-sorbed species are enhanced in indoor air by primary particles. The same primary emission event could produce significantly different airborne SVOC concentrations, and ultimately occupant exposures, in indoor environments with different condensed-phase reservoirs.

5 ACKNOWLEDGEMENTS

This work was supported by the Alfred P. Sloan Foundation Program on Chemistry of Indoor Environments via Grants G-2016-7050, G-2017-9944, and G-2019-11412. The authors thank the HOMEChem science team for a successful field campaign, Atila Novoselac and Steve Bourne for their operation of the UTest house, and Robin Weber for technical assistance. D.L. acknowledges support from the National Science Foundation (grant no. DGE 1752814). K.K. acknowledges support from the Carlsberg Foundation (grant no. CF16-0624). The authors thank the occupants of the H2 residence for participating in the study. The occupants of the H2 site gave informed consent for the study, which was conducted under a protocol approved in advance by the Committee for Protection of Human Subjects for the University of California, Berkeley (Protocol #2016 04 8656).

6 SUPPORTING INFORMATION

SV-TAG sampling conditions; SV-TAG data analysis; HR-ToF-AMS instrument operation; gaseous SVOC modeling; SVOC bin summary statistics; SVOC bin time series; SVOC bin versus temperature and $PM_{2.5}$ concentrations, SVOC bin gas-particle partitioning, SVOC bin indoor/outdoor ratios, HOMEChem siloxane concentrations, siloxane physicochemical properties

7 REFERENCES

1. Weschler, C. J.; Nazaroff, W. W. Semivolatile organic compounds in indoor environments. *Atmos. Environ.* **2008**, *42*, 9018–9040.
2. Rudel, R. A.; Perovich, L. J. Endocrine disrupting chemicals in indoor and outdoor air. *Atmos. Environ.* **2009**, *43*, 170–181.
3. Cohen, A. J.; Brauer, M.; Burnett, R.; Anderson, H. R.; Frostad, J.; Estep, K.; Balakrishnan, K.; Brunekreef, B.; Dandona, L.; Dandona, R.; Feigin, V.; Freedman, G.; Hubbell, B.; Jobling, A.; Kan, H.; Knibbs, L.; Liu, Y.; Martin, R.; Morawska, L.; Pope III, C. A.; Shin, H.; Straif, K.; Shaddick, G.; Thomas, M.; van Dingenen, R.; van Donkelaar, A.; Vos, T.; Murray, C. J. L.; Forouzanfar, M. H. Estimates and 25-year trends of the global burden of disease attributable to ambient air pollution: an analysis of data from the Global Burden of Diseases Study 2015. *Lancet* **2017**, *389*, 1907–1918.
4. Wang, C.; Collins, D. B.; Arata, C.; Goldstein, A. H.; Mattila, J. M.; Farmer, D. K.; Ampollini, L.; DeCarlo, P. F.; Novoselac, A.; Vance, M. E.; Nazaroff, W. W.; Abbatt, J. P. D. Surface reservoirs dominate dynamic gas-surface partitioning of many indoor air constituents. *Sci. Adv.* **2020**, *6*, eaay8973.
5. Ampollini, L.; Katz, E. F.; Bourne, S.; Tian, Y.; Novoselac, A.; Goldstein, A. H.; Lucic, G.; Waring, M. S.; DeCarlo, P. F. Observations and contributions of real-time indoor ammonia concentrations during HOMEChem. *Environ. Sci. Technol.* **2019**, *53*, 8591–8598.
6. Collins, D. B.; Hems, R. F.; Zhou, S.; Wang, C.; Grignon, E.; Alavy, M.; Siegel, J. A.; Abbatt, J. P. D. Evidence for gas-surface equilibrium control of indoor nitrous acid. *Environ. Sci. Technol*. **2018**, *52*, 12419–12427.
7. Kristensen, K.; Lunderberg, D. M.; Liu, Y; Misztal, P. K.; Tian, Y.; Arata, C.; Nazaroff, W. W.; Goldstein, A. H. Sources and dynamics of semivolatile organic compounds in a single-family residence in northern California. *Indoor Air* **2019**, *29*, 645–655.
8. Lunderberg, D. M.; Kristensen, K.; Liu, Y.; Misztal, P. K.; Tian, Y.; Arata, C.; Wernis, R.; Kreisberg, N.; Nazaroff, W. W.; Goldstein, A. H. Characterizing airborne phthalate concentrations and dynamics in a normally occupied residence. *Environ. Sci. Technol.* **2019**, *53*, 7337–7346.
9. Weschler, C. J.; Nazaroff, W. W. Growth of organic films on indoor surfaces. *Indoor Air* **2017**, *27*, 1101–1112.
10. Cox, S. S.; Little, J. C.; Hodgson, A. T. Predicting the emission rate of volatile organic compounds from vinyl flooring. *Environ. Sci. Technol.* **2002**, *36*, 709–714.
11. Xu, Y.; Zhang, Y. An improved mass transfer based model for analyzing VOC emissions from building materials. *Atmos. Environ.* **2003**, *37*, 2497–2505.
12. Xu, Y.; Little, J. C. Predicting emissions of SVOCs from polymeric materials and their interaction with airborne particles. *Environ. Sci. Technol.* **2006**, *40*, 456–461.

13. Xu, Y.; Cohen Hubal, E. A.; Clausen, P. A.; Little, J. C. Predicting Residential Exposure to Phthalate Plasticizer Emitted from Vinyl Flooring: A Mechanistic Analysis. *Environ. Sci. Technol.* **2009**, *43*, 2374–2380.
14. Clausen, P. A.; Liu, Z.; Kofoed-Sørensen, V.; Little, J.; Wolkoff, P. Influence of temperature on the emission of di-(2-ethylhexyl)phthalate (DEHP) from PVC flooring in the emission cell FLEC. *Environ. Sci. Technol.* **2012**, *46*, 909–915.
15. Pankow, J. F. An absorption model of gas/particle partitioning of organic compounds in the atmosphere. *Atmos. Environ.* **1994**, *28*, 185–188.
16. Goss, K.-U.; Schwarzenbach, R. P. Gas/solid and gas/liquid partitioning of organic compounds: critical evaluation of the interpretation of equilibrium constants. *Environ. Sci. Technol***. 1998**, *32*, 2025–2032.
17. Lyng, N. L.; Clausen, P. A.; Lundsgaard, C.; Andersen, H. V. Modelling the impact of room temperature on concentrations of polychlorinated biphenyls (PCBs) in indoor air. *Chemosphere* **2016**, *144*, 2127–2133.
18. Salthammer, T.; Goss, K.-U. Predicting the gas/particle distribution of SVOCs in the indoor environment using poly parameter linear free energy relationships. *Environ. Sci. Technol.* **2019,** *53*, 2491–2499.
19. Liu, C.; Morrison, G. C.; Zhang, Y. Role of aerosols in enhancing SVOC flux between air and indoor surfaces and its influence on exposure. *Atmos. Environ*. **2012**, *55*, 347–356.
20. Benning, J. L.; Liu, Z.; Tiwari, A.; Little, J. C.; Marr, L. C. Characterizing gas-particle interactions of phthalate plasticizer emitted from vinyl flooring. *Environ. Sci. Technol.* **2013**, *47*, 2696–2703.
21. Lazarov, B.; Swinnen, R.; Poelmans, D.; Spruyt, M.; Goelen, E.; Covaci, A.; Stranger, M. Influence of suspended particles on the emission of organophosphate flame retardant from insulation boards. *Environ. Sci. Pollut. Res.* **2016**, *23*, 17183–17190.
22. Wu, Y.; Eichler, C. M. A.; Cao, J.; Benning, J.; Olson, A.; Chen, S.; Liu, C.; Vejerano, E. P.; Marr, L. C.; Little, J. C. Particle/gas partitioning of phthalates to organic and inorganic airborne particles in the indoor environment. *Environ. Sci. Technol*. **2018**, *52*, 3583–3590.
23. Eriksson, A. C.; Andersen, C.; Krais, A. M.; Nøjgaard, J. K.; Clausen, P.-A.; Gudmundsson, A.; Wierzbicka, A.; Pagels, J. Influence of airborne particles' chemical composition on SVOC uptake from PVC flooring — Time-resolved analysis with aerosol mass spectrometry. *Environ. Sci. Technol.* **2019**, *54*, 85–91.
24. Collins, D. B.; Wang, C.; Abbatt, J. P. D. Selective uptake of third-hand tobacco smoke components to inorganic and organic aerosol particles. *Environ. Sci. Technol.* **2018**, *52*, 13195–13201.
25. DeCarlo, P. F.; Avery, A. M.; Waring, M. S. Thirdhand smoke uptake to aerosol particles in the indoor environment. *Sci. Adv.* **2018**, *4*, eaap8368.
26. Farmer, D. K.; Vance, M. E.; Abbatt, J. P. D.; Abeleira, A.; Alves, M. R.; Arata, C.; Boedicker, E.; Bourne, S.; Cardoso-Saldaña, F.; Corsi, R.; DeCarlo, P. F.; Goldstein, A. H.; Grassian, V. H.; Hildebrandt Ruiz, L.; Jimenez, J. L.; Kahan, T. F.; Katz, E. F.; Mattila, J. M.; Nazaroff, W. W.; Novoselac, A.; O'Brien, R. E.; Or, V. W.; Patel, S.; Sankhyan, S.; Stevens, P. S.; Tian, Y.; Wade, M.; Wang, C.; Zhou, S.; Zhou, Y. Overview of HOMEChem: House Observations of Microbial and Environmental Chemistry. *Environ. Sci.: Processes Impacts* **2019**, *21*, 1280–1300.

27. Zhao, Y.; Kreisberg, N. M.; Worton, D. R.; Teng, A. P.; Hering, S. V.; Goldstein, A. H. Development of an *in situ* thermal desorption gas chromatography instrument for quantifying atmospheric semi-volatile organic compounds. *Aerosol Sci. Technol.* **2013**, *47*, 258–266.
28. Kreisberg, N. M.; Worton, D. R.; Zhao, Y.; Isaacman, G.; Goldstein, A. H.; Hering, S. V. Development of an automated high-temperature valveless injection system for online gas chromatography. *Atmos. Meas. Tech.* **2014**, *7*, 4431–4444.
29. Isaacman, G.; Kreisberg, N. M.; Yee, L. D.; Worton, D. R.; Chan, A. W. H.; Moss, J. A.; Hering, S. V.; Goldstein, A. H. Online derivatization for hourly measurements of gas- and particle-phase semi-volatile oxygenated organic compounds by thermal desorption aerosol gas chromatography (SV-TAG). *Atmos. Meas. Tech.* **2014**, *7*, 4417–4429.
30. Isaacman-VanWertz, G.; Sueper, D. T.; Aikin, K. C.; Lerner, B. M.; Gilman, J. B.; de Gouw, J. A.; Worsnop, D. R.; Goldstein A. H. Automated single-ion peak fitting as an efficient approach for analyzing complex chromatographic data. *J. Chromatogr. A* **2017**, *1529*, 81–92.
31. Patel, S.; Sankhyan. S.; Boedicker, E.; DeCarlo, P. F.; Farmer, D. K.; Goldstein, A. H.; Katz, E. F.; Nazaroff, W. W.; Tian, Y.; Vanhanen, J.; Vance, M. E. Indoor particulate matter during HOMEChem: Concentrations, size distributions, and exposures. Submitted.
32. Tian, Y.; Arata, C.; Boedicker, E.; Lunderberg, D. M.; Patel, S.; Sankhyan, S.; Kristensen, K.; Misztal, P. K.; Farmer, D. K.; Vance, M.; Novoselac, A.; Nazaroff, W. W; Goldstein, A. H. Indoor emissions of total and fluorescent supermicron particles during HOMEChem, Submitted.
33. Hu, M.; Peng, J.; Sun, K.; Yue, D.; Guo, S.; Wiedensohler, A.; Wu, Z. Estimation of size-resolved ambient particle density based on the measurement of aerosol number, mass, and chemical size distributions in the winter in Beijing. *Environ. Sci. Technol.* **2012**, *46*, 9941–9947.
34. Zhou, J.; Chen, A.; Cao, Q.; Yang, B.; Chang, V. W.-C.; Nazaroff, W. W. Particle exposure during the 2013 haze in Singapore: Importance of the built environment. *Build. Environ.* **2015**, *93*, 14–23.
35. Little, J. C.; Weschler, C. J.; Nazaroff, W. W.; Liu, Z.; Cohen Hubal, E. A.; Rapid methods to estimate potential exposure to semivolatile organic compounds in the indoor environment. *Environ. Sci. Technol.* **2012**, *46*, 11171–11178.
36. Liu, C.; Shi, S.; Weschler, C.; Zhao, B.; Zhang, Y. Analysis of the dynamic interaction between SVOCs and airborne particles. Aerosol Sci. Technol. **2013**, *47*, 125-136.
37. Chickos, J. S.; Hanshaw, W. Vapor pressures and vaporization enthalpies of the *n*-alkanes from C_{21} to C_{30} at T = 298.15 K by correlation gas chromatography. *J. Chem. Eng. Data* **2004**, *49*, 77–85.
38. Růžička, K.; Majer, V. Simultaneous treatment of vapor pressures and related thermal data between the triple and normal boiling temperatures for *n*-alkanes C_5−C_{20}. *J. Phys. Chem. Ref. Data* 1994, *23*, 1−39.
39. Jimenez, J. L.; Canagaratna, M. R.; Donahue, N. M.; Prevot, A. S. H.; Zhang, Q.; Kroll, J. H.; DeCarlo, P. F.; Allan, J. D.; Coe, H.; Ng, N. L.; Aiken, A. C.; Docherty, K. S.; Ulbrich, I. M.; Grieshop, A. P.; Robinson, A. L.; Duplissy, J.; Smith, J. D.; Wilson, K. R.; Lanz, V. A.; Hueglin, C.; Sun, Y. L.; Tian, J.; Laaksonen, A.; Raatikainen, T.; Rautiainen, J.; Vaattovaara, P.; Ehn, M.; Kulmala, M.; Tomlinson, J. M.; Collins, D. R.; Cubison, M. J.; Dunlea, E. J.; Huffman, J. A.; Onasch, T. B.; Alfarra, M. R.; Williams, P. I.; Bower, K.; Kondo, Y.; Schneider, J.; Drewnick, F.; Borrmann, S.; Weimer, S.; Demerjian, K.; Salcedo, D.; Cottrell, L.; Griffin, R.; Takami, A.; Miyoshi, T.; Hatakeyama, S.; Shimono, A.; Sun, J. Y.; Zhang, Y.

M.; Dzepina, K.; Kimmel, J. R.; Sueper, D.; Jayne, J. T.; Herndon, S. C.; Trimborn, A. M.; Williams, L. R.; Wood, E. C.; Middlebrook, A. M.; Kolb, C. E.; Baltensperger, U.; Worsnop, D. R. Evolution of organic aerosols in the atmosphere. *Science* **2009**, *326*, 1525–1529.

40. Schauer, J. J.; Kleeman, M. J.; Cass, G. R.; Simoneit, B. R. T. Measurement of emissions from air pollution sources. 1. C_1 through C_{29} organic compounds from meat charbroiling. *Environ. Sci. Technol.* **1999**, *33*, 1566–1577.
41. McDonald, J. D.; Zielinska, B.; Fujita, E. M.; Sagebiel, J. C.; Chow, J. C.; Watson, J. G. Emissions from charbroiling and grilling of chicken and beef. *J. Air Waste Manage. Assoc.* **2003**, *53*, 185–194.
42. Robinson, A. L.; Subramanian, R.; Donahue, N. M.; Bernardo-Bricker, A.; Rogge, W. F. Source apportionment of molecular markers and organic aerosol. 3. Food cooking emissions. *Environ. Sci. Technol.* **2006**, *40*, 7820–7827.
43. Liu, Z.; Little, J. C. Semivolatile organic compounds (SVOCs): Phthalates and flame retardants. In *Toxicity of Building Materials*; Pacheco-Torgal, F., Jalali, S., Fucic, A.; Eds.; Woodhead Publishing: Oxford, **2012**; pp 122–137.
44. Bi, C.; Liang, Y.; Xu, Y. Fate and transport of phthalates in indoor environments and the influence of temperature: a case study in a test house. *Environ. Sci. Technol*. **2015**, *49*, 9674–9681.
45. Dow Corning. Home Appliances: Ovens. https://web.archive.org/web/20170705093112/http://www.dowcorning.com/content/appliance/appliancehome/Ovens.asp (retrieved on Oct. 25, 2019)